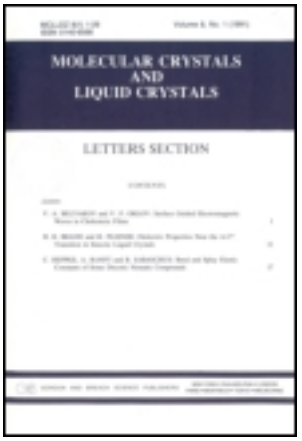

Molecular Crystals and Liquid Crystals
Publication details, including instructions for authors and subscription information:
http://www.tandfonline.com/loi/gmcl20

Influence of Sulfur Content on Cu_2ZnSnS_4 Thin Film Formation

Chan Kim [a] & Sungwook Hong [b]
[a] Department of Physics , Kyungpook National University , Daegu , 702-701 , Korea
[b] Division of Science Education , Daegu University , Gyeongsan , 712-714 , Korea
Published online: 08 Jan 2014.

To cite this article: Chan Kim & Sungwook Hong (2013) Influence of Sulfur Content on Cu_2ZnSnS_4 Thin Film Formation, Molecular Crystals and Liquid Crystals, 586:1, 147-153, DOI: 10.1080/15421406.2013.853517

To link to this article: http://dx.doi.org/10.1080/15421406.2013.853517

Mol. Cryst. Liq. Cryst., Vol. 586: pp. 147–153, 2013

ISSN: 1542-1406 print/1563-5287 online
DOI: 10.1080/15421406.2013.853517

Taylor & Francis
Taylor & Francis Group

Influence of Sulfur Content on Cu_2ZnSnS_4 Thin Film Formation

CHAN KIM[1] AND SUNGWOOK HONG[2,*]

[1]Department of Physics, Kyungpook National University, Daegu, 702-701, Korea
[2]Division of Science Education, Daegu University, Gyeongsan, 712-714, Korea

A Cu_2ZnSnS_4 (CZTS) film was formed by the sulfurization of Cu(Zn, Sn) (CZT) alloy precursors. The sulfurization was performed in evacuated and sealed quartz ampoules with various amount of supplied sulfur powder. The crystallization of the CZTS films as a function of the sulfur content was determined based on X-ray diffraction (XRD) patterns. The XRD analysis indicated that the Cu-Sn/Zn metal precursor was crystallized with various secondary phases, such as ZnS, Cu_2S, Cu_3Sn, Cu_2SnS_3, and Cu_2SnS_7. We also found that the energy gap of CZTS absorber was 1.48–1.51 eV.

Keywords Band gap energy; Cu_2ZnSnS_4; CZTS; photovoltaics; solar cell; sulfurization

Introduction

Copper-zinc-tin-chalcogenide compounds with a kesterite crystal structure are earth-abundant and have low toxicity, and they are considered promising candidates to replace Cu(In, Ga)Se_2 in thin-film solar cell applications. $Cu_2ZnSn(S, Se)_4$ have a direct band gap (Eg = 1.0–1.5 eV), large absorption coefficient (10^4 cm^{-1}), and *p*-type electrical conductivity [1–3].

Recently, CZTSe-based thin-film solar cells fabricated by a hydrazine-based solution processing showed a photovoltaic efficiency of up to 10.1% [4]. However, a photovoltaic efficiency of 7.2% was reported for CZTSSe-based solar cell devices fabricated using a colloidal nanocrystal-based process. The highest efficiency for CZTS- and CZTSe-based solar cells constructed by a vacuum process was reported to be 6.81% and 6.0%, respectively [5,6]. These results showed that CZTS- and CZTSe-based vacuum processes are possible methods of producing high-efficiency solar cell devices. In the vacuum process, the CZTS absorber with the highest conversion efficiency of 6.81% was produced by evaporating Cu, Zn, Sn and S sources [5] and CZTS absorber with 6.77% conversion efficiency was co-sputtered with three targets of Cu, ZnS and SnS [7]. To crystallize the CZTS absorber for solar cell application, only a metal precursor [5,8–11] and a precursor that already included sulfur [7,12,13] were annealed in a sulfur atmosphere. To the best of our knowledge, there are no reports on the influence that the metal-only precursor and precursor with sulfur have

*Address correspondence to Prof. Sungwook Hong, Division of Science Education, Daegu University, Jillyang, Gyeongsan, Gyeongbuk, 712-714, Korea (ROK). Tel.: (+82)53-850-6976; Fax: (+82)53-850-6979. E-mail: swhong@daegu.ac.kr

on the crystallization of CZTS absorber. This study examined the effect of sulfur content on the crystallization of CZTS absorbers.

Experimental

CZTS thin films were grown by sulfurization in evacuated and sealed ampoules. A metal precursor of CZTS absorber was deposited onto soda-lime glass through the RF magneto sputtering method. A copper-tin (Cu-Sn) layer was co-sputtered onto a zinc (Zn) layer, which was sputtered onto soda-lime glass. It has been reported that the surface morphology of metal precursor is an important parameter for improving the conversion efficiency of a solar cell [14]. This order of Zn layers on the Cu-Sn co-sputtered layer had very good surface morphology [15], but this order resulted in many voids [16] after CZTS crystallization. These voids were caused by the higher mobility of Cu than that of Zn and Sn [17]. Further, the Cu-Sn/Zn/glass layer order used in this study showed a good surface morphology [15].

Zn was sputtered for 30 min at an RF power of 135 W onto soda-lime glass. Subsequently, Cu and Sn were co-sputtered for 30 min at RF powers of 90 W and 100 W, respectively. These RF powers and deposition times were used to estimate the stoichiometry of the metal precursor. The background pressure of the chamber was less than 6.0×10^{-7} Torr. The metal precursor was deposited under an argon gas pressure of 5.5×10^{-3} Torr with a flow rate of 10 sccm. Next, the metal precursor was sulfurized in evacuated and sealed quartz ampoules with an internal volume of 14–16 cm^3 as a function of the sulfur powder content ranging from 0.0 to 4.0 mg in steps of 0.5 mg. The ampoules, which included sulfur powder and the metal precursor (12.5 cm × 25.0 cm), were annealed at of 450 °C in a furnace. The annealing temperature was increased from room temperature to annealing temperature of 450 °C for 30 min. CZTS film was annealed for 30 min. at 450 °C and allowed to cool naturally for 12 h. After annealing the CZTS, there was sulfur remaining on the inner wall of the ampoules with supplied sulfur content of more than 2.0 mg. This meant that excess sulfur content was supplied for CZTS crystallization in the ampoules.

The surface morphology, chemical composition, crystalline properties, and optical properties of the CZTS film were analyzed by scanning electron microscopy (SEM, Hitachi S-4200), inductively coupled plasma spectrometry (ICP, Optima 7300DV), X-ray diffraction (XRD, PANalytical X'pert Pro-MPD goniometer), and UV-Vis-NIR spectrometry (Carry 5000), respectively.

Results and Discussion

As shown in Fig. 1, the crystallization of the CZTS film as a function of supplied sulfur content in the quartz ampoules was observed by XRD. Figure 1(a) shows the XRD patterns of annealed CZTS films with supplied sulfur content from 0.0 mg (without sulfur content) to 1.5 mg in steps of 0.5 mg. The main peaks in the metal precursor were the alloy peaks of Cu and Sn which suggested that they were crystallized during the co-sputtering of Cu and Sn. In the XRD pattern of the sample annealed without sulfur (0.0 mg), $Cu_{6.25}Sn_5$ and Cu_5Zn_8 phases were shown. This result agrees with previous observation that Sn and Zn react preferentially with Cu [18,19]. However, Cu reacts preferentially with S over Sn and Zn in the XRD pattern of CZTS with supplied with 0.5 mg of sulfur. Cu_2S, ZnS, Cu_2SnS_3 and Cu_3Sn phases are shown instead of $Cu_{6.25}Sn_5$ and Cu_5Zn_8 phases. Sn peaks disappeared, $Cu_2Sn_3S_7$ peaks appeared, and Cu_2SnS_3 peaks were more prominent in the XRD pattern of the CZTS supplied with 1.0 mg of sulfur. In addition, more Cu_2S and ZnS peaks appeared. In the XRD pattern of sample supplied with 1.5 mg of sulfur, the Cu_2SnS_3

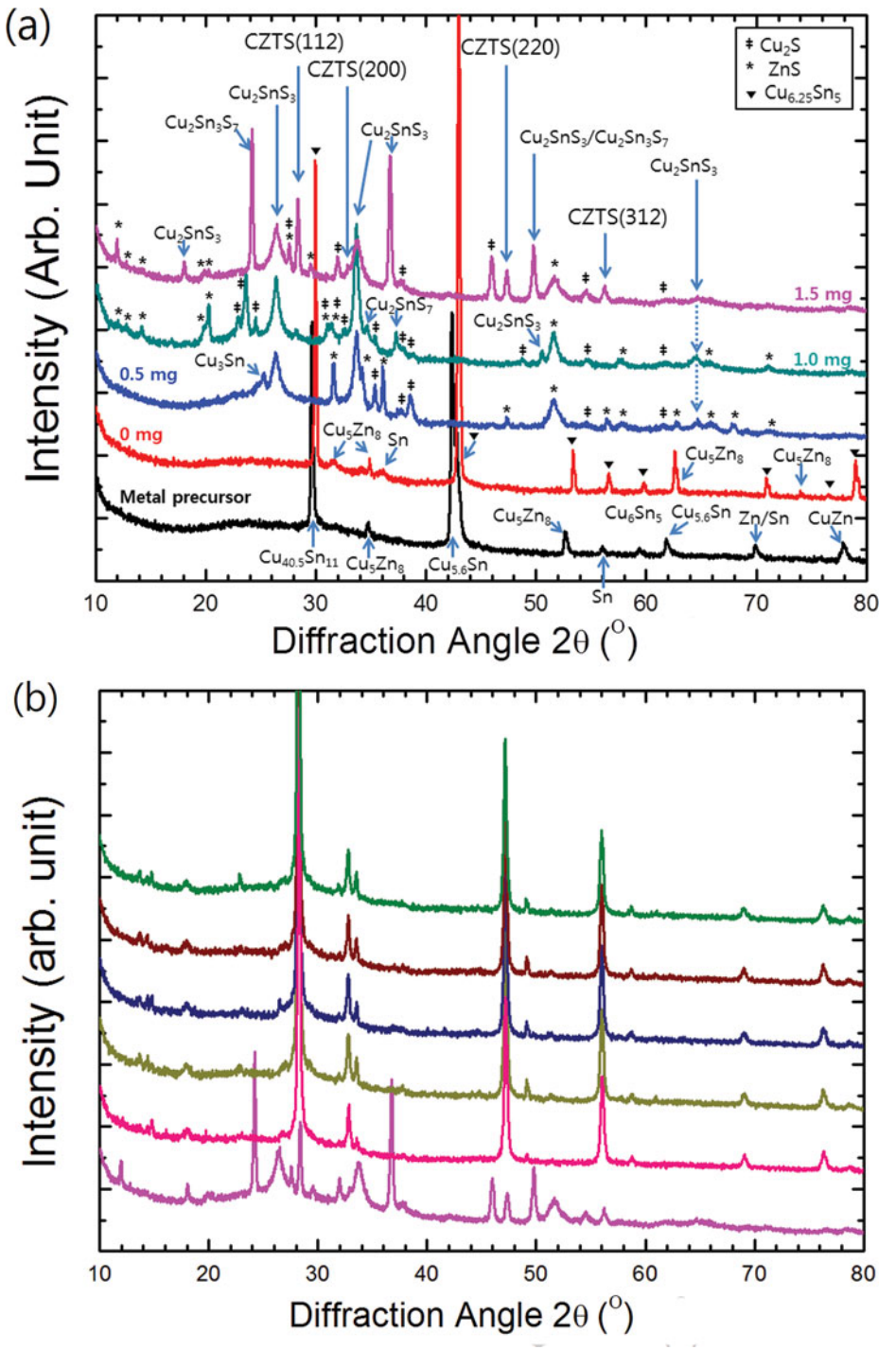

Figure 1. XRD patterns of the metal precursor, annealed CZTS films supplied with (a) less than 1.5 mg and (b) more than 1.5 mg of sulfur.

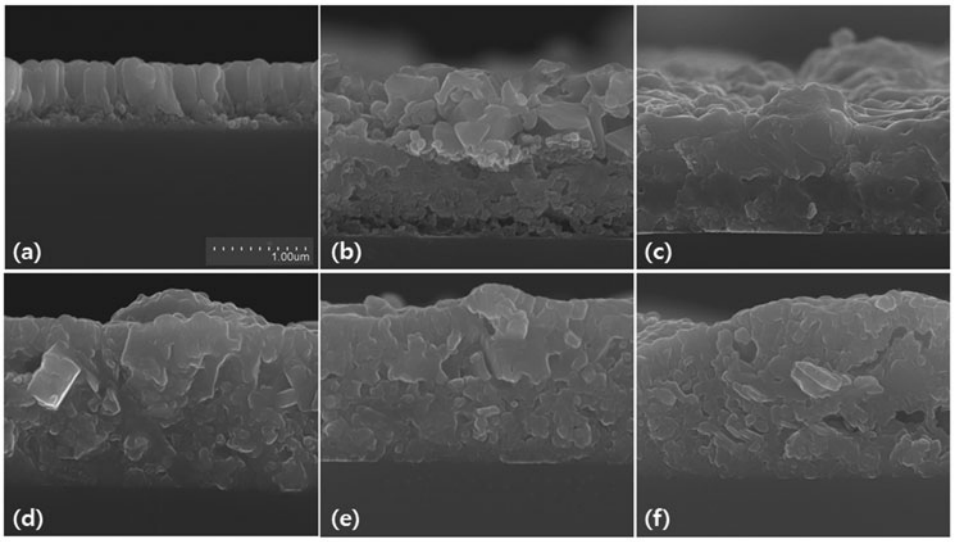

Figure 2. SEM images of the Cu_2ZnSnS_4 film annealed with supplied sulfur content of (a) 0.0 mg, (b) 2.0 mg, (c) 2.5 mg, (d) 3.0 mg, (e) 3.5 and (f) 4.0 mg.

peak was reduced, and the $Cu_2Sn_3S_7$ peak increased; however, the number of Cu_2S and ZnS peaks was reduced. In addition, the main peak of CZTS in the (112), (200), and (220) direction began to appear in the XRD pattern of the sample with 1.5 mg of sulfur. Figure 1(b) shows the XRD patterns of annealed CZTS supplied with more than 1.5 mg sulfur content. In the 2.0 mg XRD pattern, the peaks that had appeared in the 1.5 mg sample disappeared, and the CZTS peak appeared clearly. A portion of the Cu_2S, ZnS peaks still remain. There was sulfur remaining on the inner wall of the ampoules with supplied sulfur content of more than 2.0 mg. The supply of sulfur in the ampoules increased more than did the intensity of Cu_2S and ZnS peaks. This meant that excess sulfur was supplied in the annealing ampoules. From this XRD analysis, the sulfurization of Cu-Sn/Zn metal precursors a function of supplied sulfur content was according to the following process:

$$\text{1st step : Cu-Sn alloy} + S \rightarrow Cu_2S + CuSnS_3$$
$$Zn + S \rightarrow ZnS$$
$$\text{2nd step : } Cu_2S + CuSnS_3\ (\pm S) \rightarrow Cu_2Sn_3S_7$$
$$\text{3rd step : } Cu_2Sn_3S_7 + ZnS\ (\pm S) \rightarrow Cu_2ZnSnS_4$$

Figure 2 shows SEM images of the intersection of CZTS films. Figure 2(a) shows annealed metal precursor without sulfur content (0 mg). The Zn layer on glass and the Cu-Sn alloy layer were distinguishable. Figures 2(b–f) show the intersections of CZTS films with supplied sulfur contents ranging of 2.0–4.0 mg, in steps of 0.5 mg. The thickness of all is about 2.9 μm. As shown Fig. 2(b), there are many voids in the CZTS absorber (2.0 mg) and the grain size is smaller than in other absorbers. Otherwise, there are no voids in the CZTS absorbers of shown in Figs. 2(c–e), and the grain size is larger than that in Fig. 2(b) (2.0 mg). However, as shown Fig. 2(f) (4.0 mg), voids were again formed. This result means that when excess sulfur was supplied, Sn can be extracted along with sulfur in the form of SnS, resulting in a loss of Sn [20,21]. ICP analysis confirmed this result. As shown Table 1, all samples have slightly higher Cu content than stoichiometric Cu_2ZnSnS_4. From Table 1, it is clear that the Sn loss is greater with a rich sulfur supply than with a

Table 1. Chemical compositions of the CZT metal precursor and sulfurized film as a function of supplied sulfur content in the quartz ampoules

Sulfur content	Metal precursor	0 mg	2.0 mg	2.5 mg	3.0 mg	3.5 mg	4.0 mg.
Cu/(Zn+Sn)	1.21	1.24	1.20	1.21	1.28	1.25	1.26
Zn/Sn	1.00	0.98	0.99	1.00	1.01	1.03	1.05
S/Metal	0.00	0.00	0.84	0.86	1.24	1.26	1.29

poor sulfur supply. In this study, the quartz ampoules were evacuated to 10^{-3} Torr at room temperature, and sealed during sulfurization. If elements from CZTS were lost from the film in the sulfurization process, they were deposited onto the inner walls of the quartz ampoules.

The crystalline size was estimated from the XRD data using the Scherrer formula [2] as follows:

$$D = \left(\frac{0.9\lambda}{\beta cos\theta}\right), \tag{1}$$

where λ is the X-ray wavelength, β is the full width at half maximum (FWHM) in radians, and θ is the Bragg angle. Figure 3 shows the change in the crystalline size as a function of the supplied sulfur content for the (112) crystalline direction, which is the main peak in the CZTS crystal. The crystalline size increased with increasing supplied sulfur content. However, it decreased again as supplied sulfur content was exceeded 3.5 mg. This was attributed to increasing Cu_2S and ZnS crystallization and to Sn loss in the CZTS absorber due to excess supplied sulfur.

Crystallized CZTS has a tetragonal structure. The lattice constants, a and c, were calculated from the 2θ values of the (112) and (220) planes [16]. The lattice constants of the CZTS samples with 2.0 mg of supplied sulfur were determined to be $a = 5.521$ Å, c

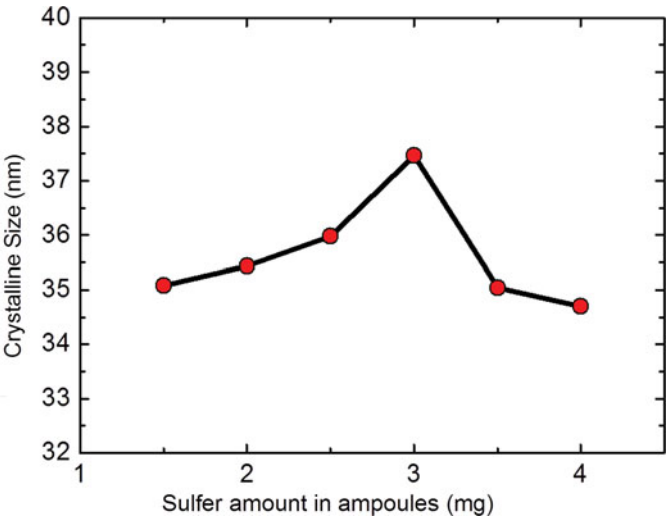

Figure 3. Change in the crystalline size in the CZTS film as a function of supplied sulfur content.

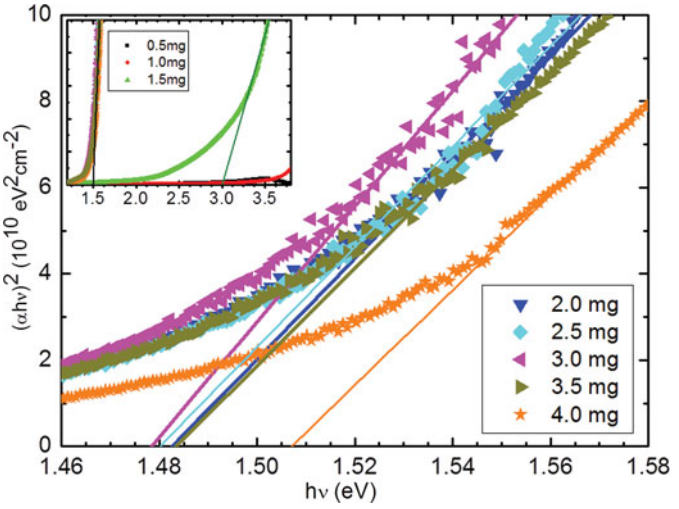

Figure 4. Plot of $(\alpha h\nu)^2$ versus photon energy $(h\nu)$ for the annealed CZTS thin film supplied with more than 2.0 mg sulfur content. Inset show that of all CZTS films.

= 10.766 Å. Other samples had similar values. The lattice constants maintained similar values to those of a CZTS single crystal, $a = 5.427$ Å, $c = 10.871$ Å, respectively [22].

The optical properties of the CZTS films were studied by UV-Vis-NIR spectroscopy (Fig. 4). The plot of $(\alpha h\nu)^2$, which is the square of the absorption coefficient (α) multiplied by the photon energy $(h\nu)$ versus $h\nu$ shows a direct band gap range of 1.48–1.51 eV. The 4.0 mg sample had a slightly greater band gap energy than that of other CZTS absorbers. This result was attributed to the increase in ZnS crystals, which have a direct band gap energy of 3.6 eV [23]. The band gap energy of the 1.5 mg sample, which had more ZnS crystal than other samples, was determined to be 3.0 eV (inset, Fig. 5).

Conclusions

A metal precursor was formulated by depositing a Cu-Sn co-sputtered layer onto a Zn layer. Quartz ampoules that included metal precursor and various amounts of sulfur content were annealed at 450 °C in a furnace. The Cu-Sn/Zn metal precursors sulfurized with various amounts of supplied sulfur content produced various secondary phases such as Cu_2S, $CuSnS_3$, ZnS, and $Cu_2Sn_3S_7$. As excess sulfur was supplied, the crystalline size of CZTS absorber decreased with increases in the secondary phases, Cu_2S and ZnS. The lattice constants of the CZTS samples were determined to be $a = 5.521$ Å, and $c = 10.766$ Å. The direct band gap energies of CZTS were 1.48–1.51 eV.

Acknowledgment

This study was supported by the Daegu University Research Grant, 2012.

References

[1] Ito, K., & Nakazawa, T. (1998). *Jpn. J. Appl. Phys.*, *27*, 2094.
[2] Rajeshmon, V. G., Kartha, C. S., Vijayakumar, K. P., Sanjeeviraja, C., Abe, T., & Kashiwaba, Y. (2011). *Solar Energy*, *85*, 249.

[3] Matsushita, H., Maeda, T., Katsui, A., & Rakizawa, T. (2000). *J. Cryst. Growth*, *208*, 416.
[4] Bag, S., Gunawan, O., Gokmen, T., Zbu, Y., Todorov, T. K., & Mitzi, D. B. (2012). *Energy Environ. Sci.*, *5*, 7060.
[5] Wang, K., Gunawan, O., Todorov, T., Shin, B., Chey, S. J., Bojarczuk, N. A., Mitzi, D., & Guha, S. (2010). *Appl. Phys. Lett.*, *97*, 143508.
[6] Grenet, L., Bernardi, S., Kohen, D., Lepoittevin, C., Noel, S., Karst, N., Brioude, A., Perraud, S., & Mariette, H. (2012). *Sol. Energy Mater. Sol. Cells*, *101*, 11.
[7] Katagiri, H., Jimbo, K., Yamada, S., Kamimura, T., Maw, W. S., Fukano, T., *et al*. (2010). *Appl. Phys. Express*, *1*, 041201.
[8] Yoo, H., & Kim, J. (2011). *Sol. Energy Mater. Sol. Cells*, *95*, 239.
[9] Araki, H., Mikaduki, A., Kubo, Y., Sata, T., Jimbo, K., Maw, W. S., Katagiri, H., Yamazaki, M., Oishi, K., & Takeuchi, A. (2008). *Thin Solid Films*, *517*, 1457.
[10] Fernandes, P. A., Salomé, P. M. P., & Cunha, A. F. (2009). *Thin Solid Films*, *517*, 2519.
[11] Liu, F., Li, Y., Zhang, K., Wang, B., Yan, C., Lai, Y., Zhang, Z., Li, J., & Liu, Y. (2010). *Sol. Energy Mater. Sol. Cells*, *94*, 2431.
[12] Platzer-Björkman, C., Scragg, J., Flammersberger, H., Kubart, T., & Edoff, M. (2012). *Sol. Energy Mater. Sol. Cells*, *98*, 110.
[13] Salomé, P. M. P., Malaquias, J., Fernandes, P. A., Ferreira, M. S., Leitão, J. P., Cunha, A. F., González, J. C., Matinaga, F. N., Ribeiro, G. M., & Viana, E. R. (2011). *Sol. Energy Mater. Sol. Cells*, *95*, 3482.
[14] Katagiri, H. (2005). *Thin Solid Films*, *480–481*, 426.
[15] Hong, S. (2012). *Mol. Cryst. Liq. Cryst.*, *565*, 153.
[16] Hong, S., Kim, C., Park, S. C., Rhee, I., Kim, D. H., & Kang, J. K. (2012). *Mol. Cryst. Liq. Cryst.*, *565*, 147.
[17] Fernandes, P. A., Salome, P. M. P., & Cunha, A. F. (2009). *Semicond. Sci. Technol.*, *24*, 105013.
[18] Wang, M. C., Yu, S. P., Chang, T. C., & Hon, M. H. (2004). *J. Alloys Compd.*, *381*, 162.
[19] Ichitsubo, T., Matsubara, E., Hujiwara, K., Yamaguchi, M., Irie, H., Kumamoto, S., & Anada, T. (2005). *J. Alloys Compd.*, *392*, 200.
[20] Redinger, A., & Siebentritt, S. (2012). *Appl. Phys. Lett.*, *97*, 092111.
[21] Redinger, A., Berg, D. M., Dale, P. J., & Siebentritt, S. J. (2011). *Am. Chem. Soc.*, *133*, 3320.
[22] Hall, S. R., Szymanski, J. T., & Stewart, J. M. (1978). *Can. Mineral.*, *16*, 131.
[23] Mail, S. S., Patil, B. M., Betty, C. A., Bhosale, P. N., Oh, Y. W., Jadkar, S. R., Devan, R. S., Ma, Y., & Patil, P. S. (2012). *Electrochim. Acta*, *66*, 216.